Human Argonaute2 and Argonaute3 are catalytically activated by different lengths of guide RNA

Mi Seul Park[a,b], GeunYoung Sim[b,c], Audrey C. Kehling[a], and Kotaro Nakanishi[a,b,c,1]

[a]Department of Chemistry and Biochemistry, The Ohio State University, Columbus, OH 43210; [b]Center for RNA Biology, The Ohio State University, Columbus, OH 43210; and [c]Molecular, Cellular and Developmental Biology, The Ohio State University, Columbus, OH 43210

Edited by Joseph D. Puglisi, Stanford University School of Medicine, Stanford, CA, and approved September 15, 2020 (received for review July 20, 2020)

RNA interfering is a eukaryote-specific gene silencing by 20∼23-nucleotide (nt) microRNAs and small interfering RNAs that recruit Argonaute proteins to complementary RNAs for degradation. In humans, Argonaute2 (AGO2) has been known as the only slicer while Argonaute3 (AGO3) barely cleaves RNAs. Therefore, the intrinsic slicing activity of AGO3 remains controversial and a long-standing question. Here, we report 14-nt 3′ end-shortened variants of let-7a, miR-27a, and specific miR-17–92 families that make AGO3 an extremely competent slicer, increasing target cleavage up to ∼82-fold in some instances. These RNAs, named cleavage-inducing tiny guide RNAs (cityRNAs), conversely lower the activity of AGO2, demonstrating that AGO2 and AGO3 have different optimum guide lengths for target cleavage. Our study sheds light on the role of tiny guide RNAs.

RNAi | Argonaute | noncoding RNA | enzyme

MicroRNAs (miRNAs) are small noncoding RNAs that control gene expression posttranscriptionally (1). Their sequences differ, but their lengths fall within a range of 20∼23 nucleotides (nt) because the precursor miRNAs are processed by Dicer, which is a molecular ruler that generates size-specific miRNA duplexes (2, 3). After those duplexes are loaded into Argonaute (AGO) proteins, one of the two strands is ejected while the remaining strand (guide) and the AGO form the RNA-induced silencing complex (RISC) (4). Therefore, the 20∼23-nt length is the hallmark of intact miRNAs. This size definition has been exploited as the rationale for eliminating ∼18-nt RNAs when AGO-bound miRNAs are analyzed by RNA sequencing (RNAseq). However, RNAseq without a size exclusion reported a substantial number of ∼18-nt RNAs bound to AGOs (5, 6). Such tiny guide RNAs (tyRNAs) are abundant in extracellular vesicles of plants (7), but little is known about their roles or biogenesis pathways. In mammals, the roles of tyRNAs are even more enigmatic.

The goal of this study was to understand target-RNA cleavage by human AGOs. In 2004, two groups reported that only AGO2 showed the guide-dependent target cleavage in vitro (8, 9). Since then, AGO1, AGO3, and AGO4 were thought to be deficient in RNA cleavage, even though AGO2 and AGO3 share the same catalytic tetrad, Asp–Glu–Asp–His, that is missing in the other human AGOs (10). Recently, we revealed that specific miRNAs such as miR-20a make AGO3 a slicer, but the activity was much lower than that of AGO2 (11). Therefore, it remained unclear whether AGO3 becomes a highly competent slicer. We revisited this long-standing question by investigating the effect of the guide length on target cleavage and discovered the unexpected role of tyRNAs in the AGO3 activation.

Results

Recombinant proteins of AGO2 and AGO3 (11) were pre-incubated with a different-length single-stranded synthetic miR-20a whose 3′ 7∼15 nt are deleted (12), followed by addition of a cap-labeled target RNA (Fig. 1*A*). While AGO2 reduced slicing activity with shorter guides, AGO3 showed the highest cleavage activity with the 14-nt guide (Fig. 1*B*). Notably, the slicing activity of AGO3 with the 14-nt miR-20a was about 30-fold higher than its 23-nt intact form, which resulted in AGO3 being a comparatively efficient slicer against AGO2. Supporting this, the kinetics of target cleavage with the 14- and 23-nt guides showed opposite trends between AGO2 and AGO3 (Fig. 1*C*). These results suggest that AGO2 and AGO3 have different optimum lengths of guide RNA for target cleavage. Hereafter, tyRNAs capable of catalytically activating AGO3 are referred to as cleavage-inducing tyRNAs (cityRNAs).

Intact miRNAs of let-7a, miR-16, and miR-19b are known to activate AGO2 but not AGO3 (11). To test whether their 14-nt tyRNAs serve as cityRNAs, recombinant AGO2 and AGO3 were programmed with either of their intact miRNA or tyRNA and subsequently incubated with the cap-labeled cognate target RNA. Loading of the tyRNAs drastically decreased or ruined the slicing activity of AGO2, compared to that of their intact form (Fig. 1*D*). In contrast, not the 14-nt miR-16 or miR-19b but the 14-nt let-7a conferred extremely competent slicing activity on AGO3. To find more cityRNAs, 14-nt tyRNAs of miR-17, miR-18a, miR-19a, miR-27a, and miR-92a were tested for in vitro target cleavage. Again, AGO2 reduced slicing activity with their 14-nt tyRNAs whereas AGO3 became a remarkably competent slicer when loaded with all except for the 14-nt miR-19a (Fig. 1*D*). These results indicate that some cityRNAs make AGO3 a superior slicer compared to AGO2.

Unlike miRNA duplexes, 14-nt RNAs are too short to form stable double-stranded (ds) RNAs and thus could be loaded as a single-stranded (ss) RNA into AGOs. To test this idea, we performed a RISC maturation assay (13, 14). A 5′ radiolabeled 23-nt small interfering RNA (siRNA)-like duplex of miR-20a (p23ds) was used as a positive control, instead of a 5′ radiolabeled 14-nt ss miR-20a (p14ss) (Fig. 2*A*). As expected, the provided 23-nt duplex was detected as its single intact strand in both AGO2 and AGO3 (Fig. 2*B*). Similarly, the intact 14-nt miR-20a was detected from both AGOs (Fig. 2*B*), demonstrating that AGO2 and AGO3 can incorporate the 14-nt ssRNAs in the cell lysate. Next, those assembled RISCs were immunopurified from the cell lysate and tested for slicing activity. FLAG-AGO2 cleaved RNAs at about 30% activity when the lysate was incubated with the 23-nt siRNA-like duplex of miR-20a (23ds) (Fig. 2 *A* and *C*). In contrast, FLAG-AGO3 showed about 50% target cleavage when the 14-nt ss miR-20a (14ss) was added to the lysate (Fig. 2*C*). To confirm that the observed RNA cleavage was due to the catalytic activity of AGO3, we repeated the experiment using a catalytically dead mutant, FLAG-AGO3 (E638A) (11). This

Author contributions: K.N. designed research; M.S.P., G.Y.S., and A.C.K. performed research; M.S.P., G.Y.S., A.C.K., and K.N. analyzed data; and K.N. wrote the paper.

The authors declare no competing interest.

[1]To whom correspondence may be addressed. Email: nakanishi.9@osu.edu.

This article contains supporting information online at https://www.pnas.org/lookup/suppl/doi:10.1073/pnas.2015026117/-/DCSupplemental.

First published October 29, 2020.

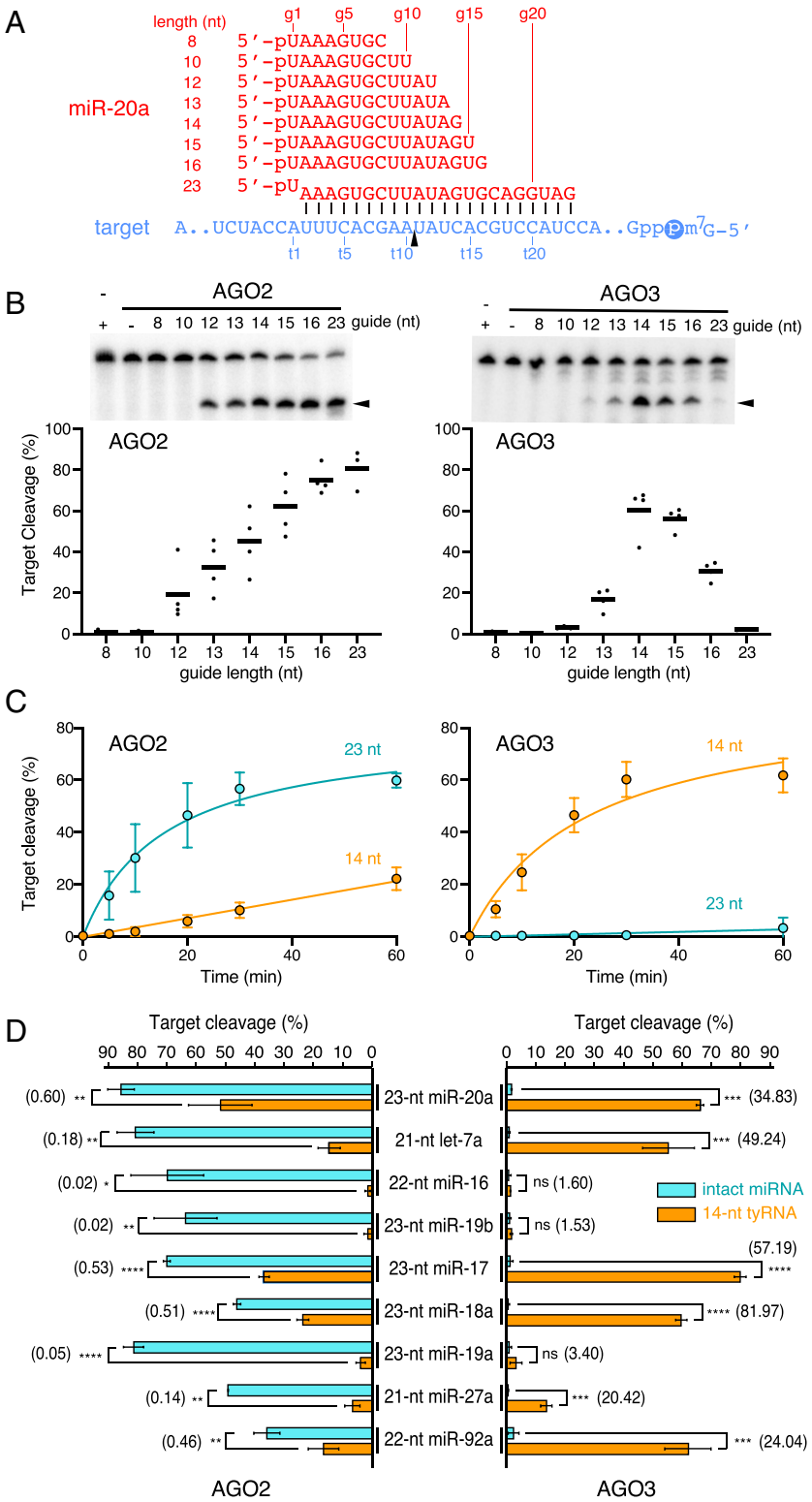

Fig. 1. The slicing activity of AGO3 is brought out by 14-nt miR-20a. (*A*) Guide (red) and target (blue) RNAs used in *B* and *C*. The 60-nt target RNAs were cap-labeled. (*B*) In vitro cleavage assay by AGO2 and AGO3 with different lengths of miR-20a. (*Top*) Representative gel images. (*Bottom*) Target cleavage percentages. Mean (bar) and individual biological replicates (dots). (*C*) Time-course assay of AGO2 and AGO3 with the 14- or 23-nt miR-20a. Mean ± SD. (*D*) In vitro target cleavage using AGO2 and AGO3 with the intact miRNAs (cyan) or 14-nt tyRNAs (orange) against their cognate targets. The numbers in parentheses indicate the relative target cleavage (fold increase) of each 14-nt tyRNA against the cognate intact miRNA. Mean ± SD. *$P < 0.05$; **$P < 0.01$; ***$P < 0.001$; ****$P < 0.0001$; ns, not significant (Student's *t* test).

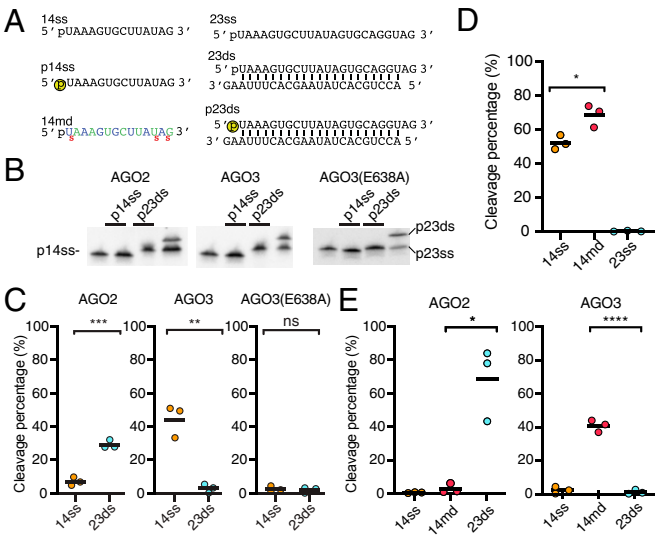

Fig. 2. In vivo loading of 14-nt single-stranded guide RNA makes AGO3 a slicer. (*A*) miR-20a variants in 14 and 23 nt; 5′-end radiolabeling is shown as a yellow circle. The 14md is identical to 14ss, except for modifications (blue: 2′-OMe, green: 2′-F, red s: phosphorothionate). (*B*) RISC assembly assay. p14ss or p23ds was added to the lysate of HEK293T cells expressing FLAG-AGO2, -AGO3, or -AGO3 (E638A). (*C*) In vitro target cleavage using AGOs programmed in cell lysate; 14ss or 23ds was added to the lysate of HEK293T cells expressing FLAG-AGO2, -AGO3, or -AGO3 (E638A). (*D*) In vitro cleavage assay of recombinant AGO3 programmed with 14ss, 14md, or 23ss. (*E*) In vitro cleavage assay using AGOs programmed within the cell; 14ss, 14md, or 23ds was transfected into HEK293T cells expressing FLAG-AGO2 or -AGO3. $*P < 0.05$; $**P < 0.01$; $***P < 0.001$; $****P < 0.0001$; ns, not significant (Student's *t* test).

mutant loaded both p14ss and p23ds to form the mature RISCs (Fig. 2 *A* and *B*) but failed to cleave RNAs (Fig. 2*C*), proving that the catalytic center of AGO3 is essential for the cityRNA-dependent target cleavage. Finally, we tested whether AGO3 incorporates 14-nt ssRNAs within the cell to assemble a functional slicer. The 14-nt ss miR-20a was modified, according to a previous report (15), to make it stable during and after transfection (14md) (Fig. 2*A*). When programmed with the 14md, the recombinant AGO3 showed a slightly higher target cleavage than with the unmodified form (Fig. 2*D*), indicating that the modified guide retained the ability to catalytically activate AGO3. Then, HEK293T cells were cotransfected with a plasmid encoding FLAG-AGO2 or FLAG-AGO3 and either the 14ss, the 14md, or the 23ds. Immunopurified FLAG-AGO2 cleaved RNA at about 70% activity with transfection of the 23ds (Fig. 2*E*). In contrast, FLAG-AGO3 cleaved the target RNA only when the 14md was cotransfected. These results demonstrate that AGO3 and 14-nt ssRNAs assemble into an active slicer in vivo.

Discussion

AGO2 cleaves any RNAs including a sequence fully complementary to the guide RNA, which means that any guide RNAs can activate AGO2. This is not the case for the AGO3 activation. Only specific tyRNAs can serve as cityRNAs due to their unique sequences. These multiple requirements extremely limit the opportunities for catalytically activating AGO3. That is why the slicing activity has not been unveiled for a long time (8, 9). Since AGO3 has retained the catalytic center throughout its molecular evolution, the cityRNA-dependent slicing activity could have a conserved role in or beyond RNA interference when all of the requirements are satisfied.

Materials and Methods

See *SI Appendix* for the extended materials and methods.

In Vitro Cleavage Assay. AGO protein (1 μM) was incubated with 100 nM 5′ phosphorylated synthetic ss guide RNA for RISC assembly in 1× Reaction Buffer, followed by addition of 100 nM 5′ cap-labeled target RNA (11).

Validation of Modified 14-nt miR-20a. Recombinant AGO3 (1 μM) was incubated with 14ss, 14md, or 23ss for 1 hour at 37 °C followed by target cleavage as described above.

In Vitro Cleavage Assay Using FLAG-AGO Programmed in the Cell Lysate. pCAGEN-FLAG-AGO (10 μg) was transfected into HEK293T cells, following our previous report (13).

In Vitro Cleavage Assay Using FLAG-AGO Programmed within the Cell. pCAGEN-FLAG-AGO (10 μg) was transfected into HEK293T cells. After 24 hours, 14ss, 14md, or 23ds was transfected. After 24 hours, the cells were harvested and sonicated following the steps in our previous report (13).

Data Availability. All study data are included in the paper and *SI Appendix*.

ACKNOWLEDGMENTS. This work was supported by a Pelotonia Fellowship (to M.S.P.), a Center for RNA Fellowship (to G.Y.S.), the NIH (R01GM124320 and R01GM138997 to K.N.), and the Office of the Director, NIH (S10OD023582).

1. D. P. Bartel, Metazoan microRNAs. *Cell* **173**, 20–51 (2018).
2. H. Zhang, F. A. Kolb, L. Jaskiewicz, E. Westhof, W. Filipowicz, Single processing center models for human Dicer and bacterial RNase III. *Cell* **118**, 57–68 (2004).
3. I. J. Macrae *et al.*, Structural basis for double-stranded RNA processing by Dicer. *Science* **311**, 195–198 (2006).
4. K. Nakanishi, Anatomy of RISC: How do small RNAs and chaperones activate Argonaute proteins? *Wiley Interdiscip. Rev. RNA* **7**, 637–660 (2016).
5. C. Kuscu *et al.*, tRNA fragments (tRFs) guide Ago to regulate gene expression post-transcriptionally in a Dicer-independent manner. *RNA* **24**, 1093–1105 (2018).
6. P. Kumar, J. Anaya, S. B. Mudunuri, A. Dutta, Meta-analysis of tRNA derived RNA fragments reveals that they are evolutionarily conserved and associate with AGO proteins to recognize specific RNA targets. *BMC Biol.* **12**, 78 (2014).
7. P. Baldrich *et al.*, Plant extracellular vesicles contain diverse small RNA species and are enriched in 10- to 17-nucleotide "tiny" RNAs. *Plant Cell* **31**, 315–324 (2019).
8. J. Liu *et al.*, Argonaute2 is the catalytic engine of mammalian RNAi. *Science* **305**, 1437–1441 (2004).
9. G. Meister *et al.*, Human Argonaute2 mediates RNA cleavage targeted by miRNAs and siRNAs. *Mol. Cell* **15**, 185–197 (2004).
10. K. Nakanishi, D. E. Weinberg, D. P. Bartel, D. J. Patel, Structure of yeast Argonaute with guide RNA. *Nature* **486**, 368–374 (2012).
11. M. S. Park *et al.*, Human Argonaute3 has slicer activity. *Nucleic Acids Res.* **45**, 11867–11877 (2017).
12. D. M. Dayeh, B. C. Kruithoff, K. Nakanishi, Structural and functional analyses reveal the contributions of the C- and N-lobes of Argonaute protein to selectivity of RNA target cleavage. *J. Biol. Chem.* **293**, 6308–6325 (2018).
13. M. S. Park *et al.*, Multidomain convergence of Argonaute during RISC assembly correlates with the formation of internal water clusters. *Mol. Cell* **75**, 725–740.e6 (2019).
14. S. Iwasaki, Y. Tomari, Reconstitution of RNA interference machinery. *Methods Mol. Biol.* **1680**, 131–143 (2018).
15. W. F. Lima *et al.*, Single-stranded siRNAs activate RNAi in animals. *Cell* **150**, 883–894 (2012).